CrystEngComm

Concentration Dependent Properties of Amorphous Carbon Nanotubes/Silica Composites via Sol-gel Technique

Journal:	*CrystEngComm*
Manuscript ID:	CE-ART-05-2014-001083.R1
Article Type:	Paper
Date Submitted by the Author:	30-Jun-2014
Complete List of Authors:	YUSOF, YUSLIZA; University of Malaya, Department of Mechanical Engineering Johan, Mohd Rafie; University of Malaya, Department of Mechanical Engineering

Concentration Dependent Properties of Amorphous Carbon Nanotubes/Silica Composites via Sol-gel Technique

Yusliza Yusof [*], *Mohd Rafie Johan*

Nanomaterials Engineering Research Group

Advanced Materials Research Laboratory, Department of Mechanical Engineering,

University of Malaya, Lembah Pantai, Kuala Lumpur, 50603 Malaysia.

Abstract

Amorphous carbon nanotubes (α-CNTs)/silica composites were synthesized by sol-gel technique. Fourier transform infrared spectroscopy (FTIR) reveals the formation of α-CNTs/silica gel network through covalent bonding. The ultraviolet-visible (UV-Vis) spectroscopy shows a strong absorption band of the composites near UV region. The amorphous structures of the composites are confirmed by X-ray diffraction (XRD) broad peaks. Field-emission scanning electron microscope (FESEM) and transmission electron microscope (TEM) show the smooth surface at lower weight percentage (wt%) of α-CNTs but rough surface at higher wt% of α-CNTs. The dielectric properties of the composites have slightly improved by incorporating α-CNTs in the silica.

Keywords: Amorphous carbon nanotubes; sol-gel; silica; composites; dielectric properties

1. Introduction

Carbon nanotubes (CNTs) have been recognized as fascinating nanomaterials due to their unique structures that gives extraordinary mechanical strength, excellent electrical and electronic properties, efficient thermal conductivity, as well as unique magnetic and optical properties [1-3].

Recently, amorphous carbon nanotubes (α-CNTs) have received much attention due to their simple synthesis process at low temperature and large yield of production [2-4]. α-CNTs are unique due to their straight tubular shape that consists of small graphene sheets with totally amorphous carbon that are roughly parallel to the tube axis [5]. They have both sp^2 and sp^3 bonding and contain parts of the properties of both diamond and graphite, which distinguish their properties from crystalline single-walled (SWNT) and multi-walled carbon nanotubes (MWNT) [2-5]. In comparison, the α-CNTs also have extraordinary wide interlayer spacing (0.40-0.44 nm) in their walls with no graphitic stacking that may offer their unique adsorption activity for small gaseous molecules [6]. In addition, the wall of α-CNTs has no chirality problem and their defects on the amorphous walls can be potentially developed for application as gaseous adsorbent and catalyst supports, field emitters, and electronic nanodevices [3-7].

To date, various fundamental researches have concerned on the development of CNTs-based composites by combining the properties of organic and inorganic components. In particular, organic components can be impregnated in the host matrix made of inorganic structure (silica, titania, etc) or a hybrid skeleton (siloxane-metal oxide hybrids, organosilicas, etc.) [8]. These composites can be implemented to new features such as excellent mechanical strength and good thermal stability. In such materials are promising to overcome some drawbacks of organic polymers such as aging, limited temperature range, degradation under high optical flux, etc. [9]. This composite may offer favourable

applications in wide areas such as optics, electronics, ionics, mechanics, sensors, catalysis, medicine, biotechnology, etc. [8-9].

Sol-gel method is a well-known process for the fabrication of inorganic composites, including in the glass formation. Silica derived sol-gel materials provides an excellent dielectric properties and outstanding thermal stability due to the skeletal network structure of silicon dioxide (SiO_2) with ultra low-*k* values ($k < 2.0$) [10]. Other work also focused on carbon nanofillers such as carbon black dispersed in silica materials prepared by the sol gel route to ascribe their electrical properties with excellent chemical and temperature stabilities [11]. This method is very versatile and attractive to incorporate CNTs in silica glasses at low temperature procedure because CNTs' oxidation would take place under temperature of 800°C in ambient atmosphere, much lower than the melting temperature of traditional silica glass [12].

Several works have described the preparation of embedded crystalline CNTs in silica matrices by a sol-gel method [10, 13-14]. The encapsulation of CNTs in silica can be prepared by controlling the conditions of hydrolysis and condensation of the sol gel precursor. However, CNTs agglomeration may occur in the latter stages of the procedure especially when the solvent is evaporated due to the incompatibility of CNTs with sol gel matrices [15]. The use of ultrasonication technique will improve the CNTs dispersion and increases the molecular level mixing between the CNTs and the silica network by speed up the transformation from sol to gel. Ultrasonic waves generates acoustic cavitations' bubbles that can break and restrain the agglomeration of the CNTs, obtaining a homogeneous and small size distribution of the inorganic clusters in the aerogel [16].

Incorporating α-CNTs with silica to improve their properties is the main purpose of this paper. As known, silica is a popular ceramic material having superior mechanical properties and good UV transparency. These properties make it attractive for use in many applications.

In the present study, these α-CNTs/silica composites were synthesized by using sol-gel technique and their properties were scrutinized for different wt% of α-CNTs.

2. Experimental

2.1. Sample preparation

α-CNTs were synthesized at low temperature of 200°C via a simple chemical route [2]. The as-synthesized α-CNTs were treated with concentrated hydrochloric acid (HCl) (5M), followed by methanol (CH_3OH) (99.8%) and purified water for several times. Tetraethyl orthosilicate (TEOS) was used as a precursor of silica. Silica (SiO_2) sols were prepared via modified technique [17]. Firstly, α-CNTs at different weight percentage (0.05, 0.1, 0.5 and 1.0 wt%) were dispersed in 10 ml of N, N-dimethylformamide (DMF) (99.5%), then mixed in the solution containing 12.ml of TEOS and 10 ml of ethanol. TEOS solution was initially stirred for 30 min and ultrasonicated for 60 min to inhibit any possible aggregation of α-CNTs. The solution containing 9 ml of ethanol, 18 ml of water, 0.07 ml of 35% aqueous ammonia ($NH_3.H_2O$), and 0.3 ml of 0.5 M ammonium fluoride (NH_4F) was slowly injected (1.2 ml/min) into the TEOS/α-CNTs sol. The mixed sol was kept stirred and then sonicated again for 20-30 min. The mixture was left dried at room temperature for 4 days, and 2 hours in the oven at 120 °C for removing the excess of DMF solvent. The dried mixtures were grounded into powder for further characterizations. As reference, silica sol-gel without α-CNTs was prepared in a similar approach.

2.2. Characterizations

Fourier-transform Infrared (FTIR) spectra of the α-CNTs/silica composites were recorded by using infrared spectroscopy (Perkin-Elmer Spectrum 400 spectrometer). The ultraviolet visible spectra of the α-CNTs/silica composites were recorded using UV-Vis spectrophotometer (Varian Cary Win UV 50). Structural analysis was carried out using X-ray

diffraction (XRD) (SIEMENS D5000) with Ni-filtered Cu-Kα radiation operated at 60 kV and 60 mA. The XRD patterns of the samples were collected at a Bragg's angles between 5 and 80° (2θ) in a scanning speed of 2° /min.

The morphologies of the α-CNTs/silica composites were observed using a field emission scanning electron microscope, FESEM (AURIGA, ZEISS) operated at an accelerating voltage of 1.0 kV, and transmission electron microscope, TEM (LIBRA$_{®}$ 120) operated at accelerating voltage of 120 kV. The complex permittivity of α-CNTs/silica composites was conducted by the coaxial probe method using a Agilent vector network analyser (VNA) (model 85070E). The complex permittivity was defined as $\varepsilon_r = \varepsilon' - j\varepsilon''$, where ε' is the real permittivity and ε'' is the imaginary permittivity that relates the energy storage and dissipation capabilities within materials, respectively. The complex permittivity was measured in the frequency range between 6 to 20 GHz.

3. Results and discussion

3.1 FT-IR analysis

FT-IR spectra in Fig. 1 confirm the formation of α-CNTs/silica gel network prepared by the sol-gel process. Incorporation of α-CNTs are perceived significantly affect the gross IR spectral features of the silica composites (Fig. 1(b-e)) compared to the unreinforced silica (Fig. 1a). The IR spectra reveals the presence of main vibrational modes correspond to the Si-O-Si groups that show characteristics transmittance band in the region between 400-800 cm^{-1} and a very pronounces band in the range 1000-1300 cm^{-1} [19-23]. The narrow and deep peaks appeared at ~467 cm^{-1} corresponds to the rocking vibration of the oxygens perpendicular to the Si-O-Si planes with some Si cation motion, and the small peaks appeared at ~666 cm^{-1} corresponds to the strongly polarized Si-O symmetric stretch [23]. The band in range 790 and 810 cm^{-1} is characterized by two modes of $Si-O_4$ asymmetric stretching and CH_2 rocking

[23]. The peaks observed at ~794 cm^{-1} indicate the characteristic of symmetric Si-O-Si stretch, in which the oxygen atoms move at the right angle to the Si-Si lines and in the Si-O-Si planes. While the peak appeared at ~1069 cm^{-1} is due to the characteristics of Si···O···Si asymmetric stretch [20, 24]. This peak shifted towards lower wavenumber and the intensity increased with the addition of α-CNTs in silica composites. This trend advocates that the incorporated α-CNTs are covalently bonded to the silica network through the sol-gel process.

The conversion of TEOS to silica gel is identified by the IR peaks at ~556 and 970 cm^{-1} assigned to the vibration of the Si-OH rocking and Si-OH stretching, which arise as the byproduct due to incomplete condensation of silanes [23]. The presence of Si-OH groups is identified as the silanol bonds that can form strong hydrogen-bonding between a hydrogen atom of a hydroxyl group and an oxygen atom of other hydroxyl group [20]. The sharp peak at ~1391 cm^{-1} is observed due to the $-CH_2$ scissoring of TEOS associated with very small peaks appear at band between 1400-1460 cm^{-1} that represent $-CH_3$ groups [19, 23]. The presence of carbon groups to the silicate matrix is identified in the IR spectra with pronounce sharp peaks appear in the range 1610-1680 cm^{-1}, which are attributed to C=O and C=C stretching [19-20,]. The very broad band located between 3000 and 3600 cm^{-1} is assigned to the stretching and bending of O-H group, respectively [15]. The intensity of –OH peaks located at ~3357 cm^{-1} became increased and broadened as the amount of α-CNTs also raised. This phenomenon is because the amorphous walls of nanotubes have many defects that can absorb moisture conveniently when the samples are exposed to air [2].

3.2 UV-Vis study

The UV/Vis absorption spectra of the unreinforced silica and α-CNT/silica composites are shown in Fig. 2. The spectrum of unreinforced silica in the near ultraviolet region shows a strong absorption band at 210 nm. However, the band becomes broader and shifted to 220nm, with the increasing wt% of α-CNTs. This phenomenon are observed due to the electronic energy transitions of nanotubes with increasing filler ratios and the formation of charge-transfer species as the nanotubes can be covalently bonded to the silica matrix [12]. The relative broadness of this band could be ascribed to the microspores scattering existing in the silica sol-gel and inter-particle interactions when the silica matrix adsorbed on the sidewall of the nanotubes [21]. From the spectra, it could be predicted that the α-CNTs/silica composites preserve greater transmittance stability in the near ultraviolet region [21]. This property suggests that α-CNTs/silica composites are attractive for optical utilities because of their strong absorption to near UV region.

3.3 XRD study

Fig. 3(a) shows a broad band with low intensity centered at angle of $2\theta=23°$ correspond to typical of silica from TEOS [19, 21]. Fig. 3(b-e) shows the XRD patterns of α-CNTs/silica composites similar with the unreinforced silica. However, their intensity increases and the full-width half maximum (FWHM) become less broaden with increasing wt% of α-CNTs. No other detectable characteristics peaks were found in the pattern. This result could be ascribed due to the absolute amorphous character of the α-CNTs [5].

3.4 Morphological analysis

Fig. 4a shows the micrograph of unreinforced silica with large spherical shape and non-uniform particles sizes vary from 2 to 4.5 μm. The micrograph considers a rough surface. The acid/base (pH ≥ 7.5) catalytic during sols process caused the growth of silica sols became spherical porous clusters (particles) due to further reflux reaction of TEOS [25]. The surface structures of α-CNTs/silica composites revealed a smooth and dense surface at low wt% of α-CNTs (Fig. 4b). It shows that these nanotubes exhibit a good dispersion in the silica composite films with less porosity. However, the surface micrograph at higher wt% of α-CNTs displayed roughness with a particle-like surface. The existence of pores also increased with increasing wt% of α-CNTs. This observation is due to the aggregation of the nanotubes that might occur during latter stages of the sol-gel process (Fig. 4c). The results are in good agreement with the TEM observation as shown in Fig.5.

Fig. 5 shows the TEM images of the silica and α-CNTs/silica composites. A well dispersed state of the silica sols is observed in Fig. 5a shows that the produced sol was homogeneous. The structure also seems like a bead chain network due to the acid/base catalytic sols process. The morphology of the as-synthesized α-CNTs/silica composites reveals the formation of amorphous silica coated α-CNTs (Fig. 5b). This phenomenon is ascribed due to the roughly surface and some defects existed on the amorphous carbon wall of nanotubes, which may serve as the nuclei for further silica growth. Thereby, the silica particles are highly deposited onto α-CNTs surfaces. The image however, also contains some black spots that may represent some aggregates of nanotubes with silica sols that occur during the hydrolysis of TEOS. At higher wt% of α-CNTs, a clear image of nanotube templates was found encapsulated with silica sols (Fig. 5c). The FESEM and TEM images confirm the formation of coated α-CNTs in silica network through sol-gel process as previously characterized in FTIR spectra (Fig. 1).

3.5 Dielectric analysis

Fig. 6 shows the complex permittivity spectra of all samples. As seen in Fig. 6a, the real permittivity ε′ of the silica decreases, when the frequency increases from 6 to 20 GHz. This phenomenon is mainly affected by the amount of polarization within the samples when an electrical field is applied, which causing the localized charges, i.e., electrons and protons tends to redistribute among themselves. However, the polarization effect decreased at higher frequency (X-band frequency range) because of dielectric relaxation [26]. Incorporation of α-CNTs in the silica maintained the similar decreasing trend of ε′ with increasing frequency. The value of ε′ for the composite at 1.0 wt% of α-CNTs showed no different effect on the energy storage of the unreinforced silica. The addition of α-CNTs in silica is rather dominating the dielectric loss of the composites as presented by the imaginary ε″ in Fig. 6b. The increasing trend of ε″ with increasing frequency drops off upon reaching the relaxation peak at the frequency of 12 GHz. This is because the electric field is mainly influenced by the dipole rotation when the orientation polarization disappears. It is observed with the addition of 1.0 wt% of α-CNTs in the composites have slightly reduced the energy loss, ε″ by only 2% at the frequency of 12 GHz. It is because electromagnetic waves strikes the conductive surface of nanotubes has induced conduction current due to free electrons that takes place in energy dissipation inside the samples [26]. Fig. 6c shows the loss tangent ($\tan \delta = \varepsilon''/\varepsilon'$), also called dissipation factor, D, of all samples. It seems that the loss tangent generally increased with increasing frequency, but slightly reduced with higher wt% of α-CNTs. The enhancement of complex permittivity of the α-CNTs/silica composites as low lossy materials are ascribed to the lower value of $\tan \delta$.

4. Conclusions

In summary, this work demonstrated the possibility of fabricating α-CNTs/silica composites by the sol-gel technique. Incorporation of α-CNTs are perceived significantly affect the silica network through covalent bonding of Si-O-Si and C=C groups. Absorption spectra become broader and red shifted with increasing wt% of α-CNTs. XRD patterns proved the amorphous stretch of the composites. FESEM images show that the composites exhibit a smooth and dense surface at low wt% of α-CNTs, but displayed rather rough surface at high reinforcement of α-CNTs. While TEM images revealed the microstructure of α-CNTs after being coated with the silica particles. However, the present of α-CNTs play minor role in the dielectric properties of the composites. With the addition of 1.0 wt% α-CNTs, the energy loss (ε″) was reduced by 2% at the relaxation frequency of 12 GHz. In future, the development of α-CNTs/silica composites are expected to find new light on the possible applications as field emitters, electronic nanodevices, catalyst support, energy conversion and storage materials.

Acknowledgements

The authors thanks to Ministry of Higher Education of Malaysia and University of Malaya for funding through UM/MOHE- HIR Research Grant (UM.C/HIR/MOHE/ENG/12).

References

[1] S. Iijima, Nature 354 (1991) 56-58.

[2] K.H. Tan, R. Ahmad, B.F. Leo, M.Y. Yew, B.C. Ang, M. R. Johan, Materials Research Bulletin 47 (2012) 1849-1854.

[3] L. Sun, C. Yan, Y. Chen, H. Wang, Q. Wang, J. Non-Crystalline Solids 358 (2012) 2723-2726.

[4] Jana, S.; Banerjee, D.; Jha, A.; Chattopadhyay, K. K., *Materials Research. Bulletin,* **2011**, 46, 1659-1664.

[5] L. Ci, B. Wei, C. Xu, J. Liang, D. Wu, S. Xie, W. Zhou, Y. Li, Z. Liu, D. Tang, Journal of Crystal Growth 233 (2001) 823-828.

[6] H. Nishino, C. Yamaguchi, H. Nakaoka, R. Nishida, Carbon 41 (2003) 2159-2179.

[7] Z.D. Hu, Y.F. Hu, Q. Chen, X.F. Duan, L.M. Peng, J. Phys. Chem. B 110 (2006) 8263-8267.

[8] C. Sanchez, B. Julian, P. Belleville, M. Popall, J. Mater. Chem 15 (2005) 3559-3592.

[9] L. Berguiga, J. Bellessa, F. Vocanson, E. Bernstein, J.C. Plenet, Optical Materials 28 (2006) 167-171.

[10] S. Loo, S. Idapalapati, S. Wang, l. Shen, S. G. Mhaisalkar, Scripta Materialia 57 (2007) 1157-1160.

[11] T.H. Hubert, A. Shimamura, A. Klyszcz, Materials Science-Poland 23 (2005) 61-68.

[12] Z. Hongbing, Z. Chan, C. Wenzhe, W. Minquan, Chemical Pysics Letters 411 (2005) 373-377.

[13] H. Nakamura, Y. Matsui, J. Am. Chem. Soc. 117 (1995) 2651-2652.

[14] A.J. Lopez, A. Urena, J. Rams, Materials Letters 64 (2010) 924-927.

[15] C. Zheng, M. Feng, Y. Du, H. Zhan, Carbon 47 (2009) 2889-2897.

[16] A.J. Lopez, A. Rico, J. Rodriguez, J. Rams, Applied Surface Science 256 (2010) 6375-6384.

[17] J.E. Kielbasa, J. Liu, K.B. Ucer, D.L. Carroll, R.T. Williams, J Mater Sci: Mater Elelectron 18 (2007) 435-438.

[18] Y. Chujo, KONA No.25 (2007) 255-260.

[19] M.R. Yu, G. Suyambrakasam, R/J. Wu, M. Chavali, Sensors and Actuators B 161 (2012) 938-947.

[20] H. Aguiar, J. Serra, P. Gonzalez, B. Leon, Journal of Non-Crystalline Solids 355 (2009) 475-480.

[21] C. Zheng, W. Chen, X. Ye, Optical Materials 34 (2012) 1042-1047.

[22] Z. Zhou, S. Wang, L. Lu, Y. Zhang, Y. Zhang, Composites Science and Technology 68 (2008) 1727-1733.

[23] M.C. Matos, L.M. Iiharco, R.M. Almeida, Journal of Non-Crystalline Solids 147 & 148 (1992) 232-237.

[24] N.D. Singho, M.R. Johan, Int. J. Electrochem. Sci., 7 (2012) 5604-5615.

[25] G. Wu, J. Wang, J. Shen, T. Yang, Q. Zhang, B. Zhou, Z. Deng, B. Fan, D. Zhou, F. Zhang, Materials Science and Engineering B78 (2000) 135-139.

[26] M. Mahmoodi, M. Arjamand, U. Sundaraj, S. Park, Carbon 50 (2012) 1455-1464.

AUTHOR INFORMATION

***Corresponding Author**

Phone: +603-79676873. Fax: +603-79675314. Email: yus_liza@siswa.um.edu.my

Notes

The authors declare no competing financial interest.

Figures Caption

Fig. 1. FT-IR spectra of α-CNT/silica composites with various wt% of α-CNTs: (a) 0; (b) 0.05 ; (c) 0.1 ; (d) 0.5 ; (e) 1.0 .

Fig. 2. UV-vis absorption spectra of α-CNT/silica composites with various wt% of α-CNTs: (a) 0 ; (b) 0.05 ; (c) 0.1 ; (d) 0.5 ; (e) 1.0.

Fig. 3. XRD patterns of α-CNT/silica composites with various wt% of α-CNTs: (a) 0; (b) 0.05 ; (c) 0.1 ; (d) 0.5 ; (e)1.0.

Fig. 4. FESEM images of the surface morphologies: (a) unreinforced silica; (b) 0.1 wt% α-CNTs/silica; (c) 1.0 wt% α-CNTs/silica composites.

Fig. 5. TEM images showing microstructure of the : (a) unreinforced silica (b) 0.1 wt % α-CNTs/silica; (c) 1.0 wt% α-CNTs/silica composites.

Fig. 6. Complex permittivity spectra of the α-CNTs/silica composites as a function of frequency: (a) real permittivity; (b) imaginary permittivity; (c) loss tangent.

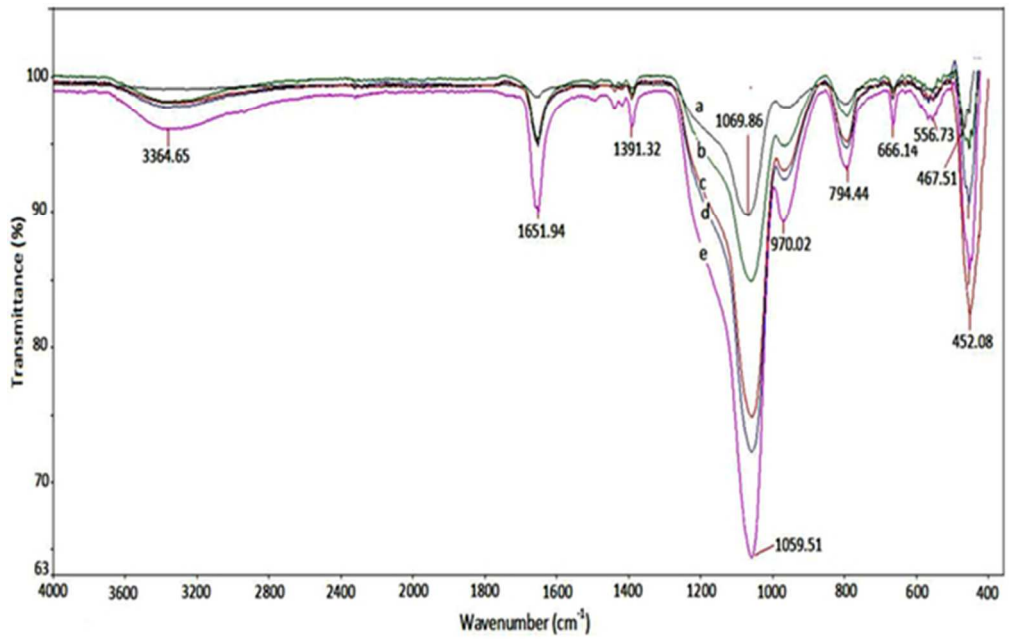

Fig. 1. FT-IR spectra of α-CNT/silica composites with various wt% of α-CNTs: (a) 0; (b) 0.05 ; (c) 0.1 ; (d) 0.5 ; (e) 1.0 .
50x32mm (300 x 300 DPI)

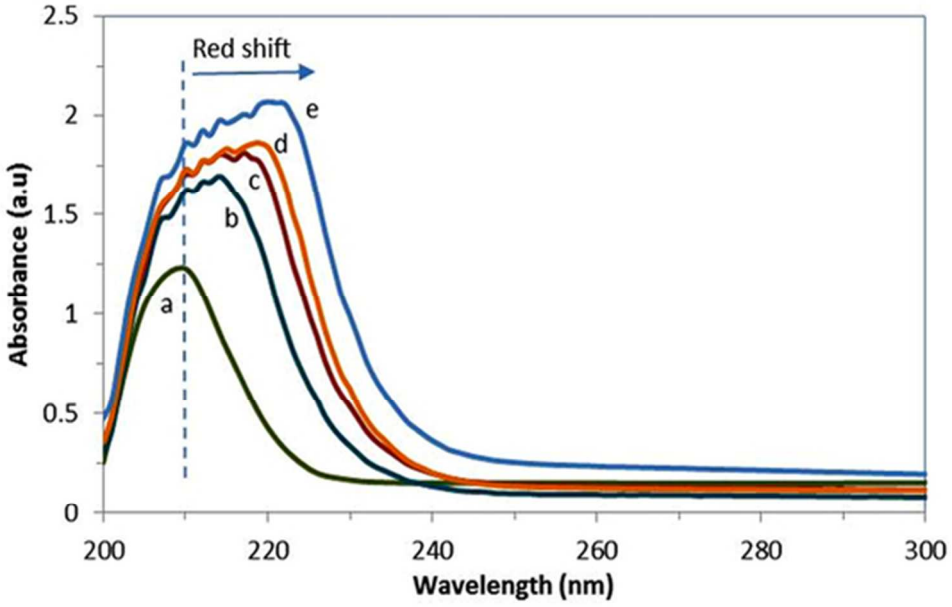

Fig. 2. UV-vis absorption spectra of α-CNT/silica composites with various wt% of α-CNTs: (a) 0 ; (b) 0.05 ; (c) 0.1 ; (d) 0.5 ; (e) 1.0.
49x31mm (300 x 300 DPI)

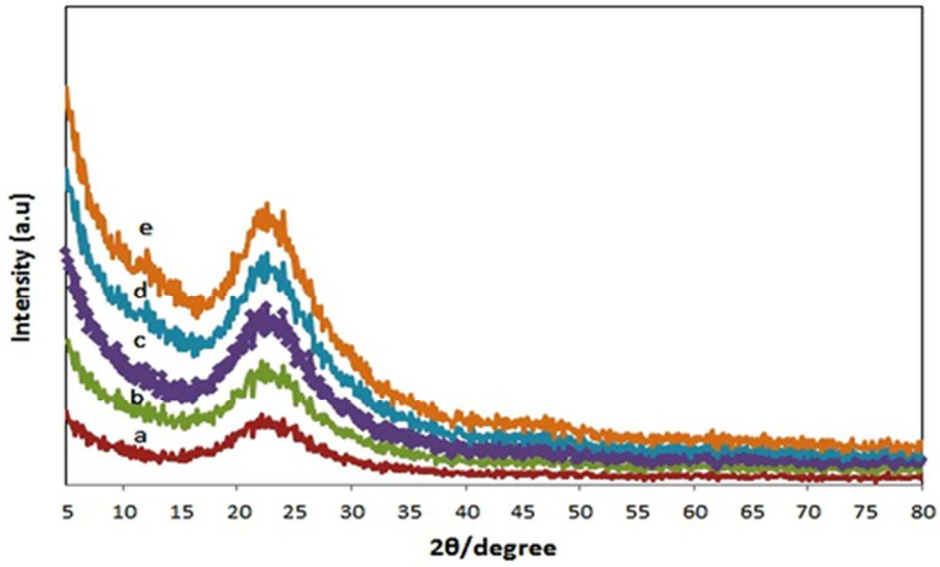

Fig. 3. XRD patterns of α-CNT/silica composites with various wt% of α-CNTs: (a) 0; (b) 0.05 ; (c) 0.1 ; (d) 0.5 ; (e)1.0.
49x31mm (300 x 300 DPI)

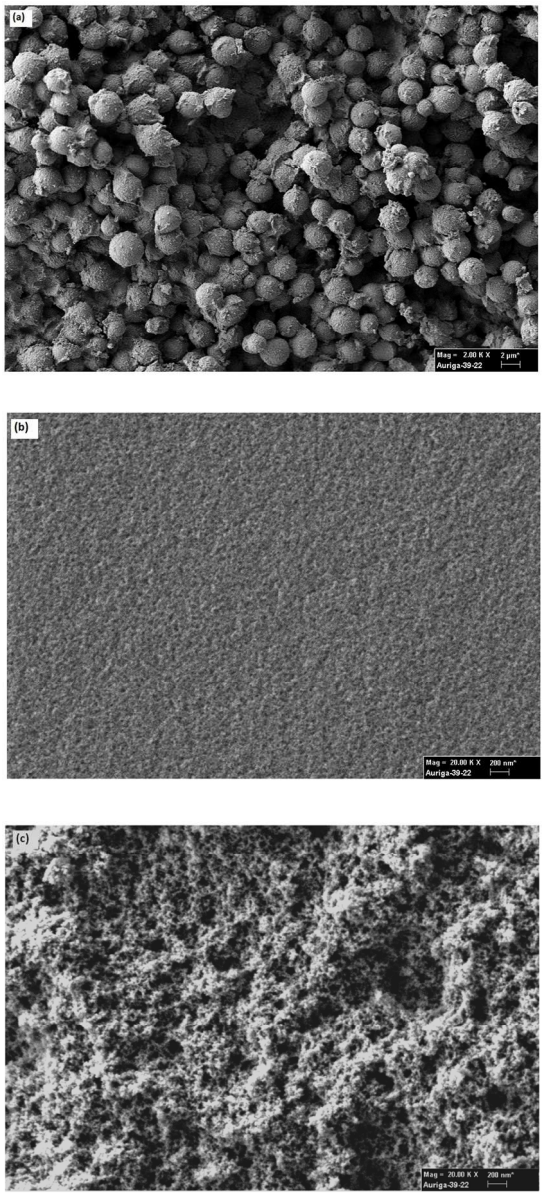

Fig. 4. FESEM images of the surface morphologies: (a) unreinforced silica; (b) 0.1 wt% α-CNTs/silica; (c) 1.0 wt% α-CNTs/silica composites.
245x545mm (300 x 300 DPI)

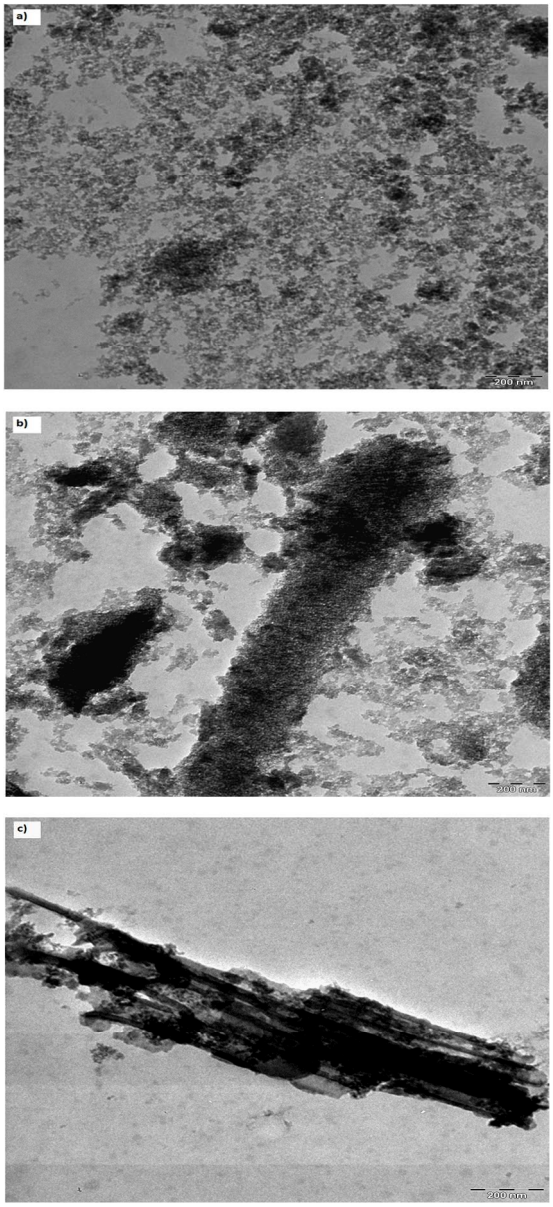

Fig. 5. TEM images showing microstructure of the : (a) unreinforced silica (b) 0.1 wt % α-CNTs/silica; (c) 1.0 wt% α-CNTs/silica composites.
244x537mm (300 x 300 DPI)